Available online at www.sciencedirect.com
ScienceDirect
European Journal of Pharmacology 559 (2007) 14–20
www.elsevier.com/locate/ejphar

2-(3-Fluorophenyl)-6-methoxyl-4-oxo-1,4-dihydroquinoline-3-carboxylic acid (YJC-1) induces mitotic phase arrest in A549 cells

Mei-Hua Hsu [a], Chun-Jen Chen [a], Sheng-Chu Kuo [a], Jing-Gung Chung [b], Ya-Yun Lai [c], Che-Ming Teng [d], Shiow-Lin Pan [d], Li-Jiau Huang [a,*]

[a] *Graduate Institute of Pharmaceutical Chemistry, China Medical University, No. 91, Hsueh-Shih Road, Taichung 40421, Taiwan (ROC)*
[b] *Graduate Institute of Medical Science, China Medical University, Taichung, Taiwan*
[c] *Department of Applied Chemistry, Chung Shan Medical University, Taichung, Taiwan*
[d] *Pharmacological Institute, College of Medicine, National Taiwan University, Taipei, Taiwan*

Received 12 June 2006; received in revised form 1 December 2006; accepted 6 December 2006
Available online 12 December 2006

Abstract

A 2-phenyl-4-quinolone (2-PQ) derivative, 2-(3-fluorophenyl)-6-methoxyl-4-oxo-1,4-dihydroquinoline-3-carboxylic acid (YJC-1), was synthesized in our laboratory. In this study, we delineated the growth-inhibitory effect of YJC-1 in human lung carcinoma A549 cells. YJC-1 inhibited cell growth with an IC_{50} value of about 4.8 μM via microtubule polymerization, causing growth arrest in the mitotic phase. Immunoblotting analysis revealed a dramatic induction of cyclin-dependent kinase (CDK) inhibitor $p21^{Cip1/Waf1}$ and down-regulation of Cdc25C phosphatase to inhibit the protein expression of cyclin B1 and CDK1. We also found that YJC-1 induced a profound time-dependent elevation in $p21^{Cip1/Waf1}$ gene expression in comparison with the negative control. *In vivo*, we also found that YJC-1 significantly suppressed tumor growth in mice inoculated with A549 cells. These findings suggest that YJC-1 can suppress A549 cell growth via mitotic phase arrest.

Keywords: 2-Phenyl-4-quinolone (2-PQ); 2-(3-Fluorophenyl)-6-methoxyl-4-oxo-1,4-dihydroquinoline-3-carboxylic acid (YJC-1); Mitotic phase arrest; Microtubule polymerization; $p21^{Cip1/Waf1}$; A549 cells

1. Introduction

Lung cancer is the leading cancer killer in the United States and in other developed countries, causing more death than the next three most common cancers combined (colon, breast, and prostate). An estimated 163,510 deaths from lung cancer will occur in the United States during 2005. The expected five-year survival rate for lung cancer patients has not improved significantly in the past 27 years (<15%) (Jemal et al., 2005). A rising death rate from lung cancer has also been observed in Taiwan. About 31.58 persons per 100,000 people died from lung cancer in Taiwan during 2004 (Department of Health, 2005). Obviously, there is an urgent need to identify new therapeutic agents for the treatment of lung cancer. Aside from surgery and radiotherapy, chemotherapy is one of the most common forms of lung cancer therapy (Osterlind, 2001).

Current rational drug development in cancer therapy appears to concentrate on the discovery of effective pharmaceutical agents that can regulate the cell cycle signaling pathway (Shapiro and Harper, 1999; Owa et al., 2001; Igor, 2003; Stewart et al., 2003). Perturbations of the cell cycle are commonly described in carcinogenesis (Marcos and Mariano, 2001). The ability of normal cells to undergo cell cycle arrest after DNA damage is crucial for the maintenance of genomic integrity. A defect in this regulation of the cell cycle results in genetic modifications that contribute to carcinogenesis (Sandal, 2004). Currently, chemotherapeutic agents used in lung cancer treatment include various drugs such as doxorubicine, paclitaxel, vincristine, and camptothecin (Osterlind, 2001). Most of these agents can reverse the aberrant cell cycle by directly inhibiting DNA synthesis, interfering with microtubule function or inhibiting topoisomerase, thereby affecting the proliferation,

* Corresponding author. Tel.: +886 4 22053366x1007; fax: +886 4 22030760.
E-mail address: ljhuang@mail.cmu.edu.tw (L.-J. Huang).

0014-2999/$ - see front matter © 2007 Published by Elsevier B.V.
doi:10.1016/j.ejphar.2006.12.001

division and apoptotic properties of cancer cells (Pizzolato and Saltz, 2003; Bacher et al., 2001; Larsen et al., 2003). In this context, 2-phenyl-4-quinolone (2-PQ) derivatives have been the subject of investigations as a new class of antitumor agents during the past 13 years (Kuo et al., 1993; Li et al., 1994a,b; Chen et al., 1997; Xia et al., 1998, 2003; Hadjeri et al., 2004). The initially synthesized 2-PQ derivatives showed promising activity, and subsequent studies investigated many substituents and substitution patterns in the A and C rings (Fig. 1). Structure-activity studies showed that substitution at the C8 and *p* positions is generally deleterious to activity, while substitution at the C6 and *m* positions is favorable to activity (Kuo et al., 1993; Li et al., 1994a,b). These effective compounds possess potent cytotoxic activity against human cancer cell lines, but all of them are too lipophilic to be optimal for *in vivo* and clinical studies. Introducing a carboxylic acid group into the 2-PQ skeleton should increase polarity and might improve the pharmacokinetic properties of these cytotoxic compounds (Lai et al., 2005). An example of these target effective compounds, 2-(3-fluorophenyl)-6-methoxyl-4-oxo-1,4-dihydroquinoline-3-carboxylic acid (YJC-1), was synthesized in our laboratory (Fig. 1). It was evaluated against a panel of 39 human cancer cell lines and showed significant activity against most cancer cell lines (Lai et al., 2005). Evaluation of the cytotoxicity data using the COMPARE computer algorithm suggests that YJC-1 shares a similar action mechanism with navelbine, vindene or paclitaxel with a possible mechanism to interfere cellular tubulin function (Lai et al., 2005). In this study, we investigated whether the antiproliferative effect of YJC-1 in A549 cells is mediated by cycle arrest in the mitotic phase. Our results indicated that YJC-1 can indeed promote mitotic arrest in A549 cells via microtubule polymerization.

2. Materials and methods

2.1. Materials

YJC-1 was synthesized in our laboratory as described by Lai et al. (2005). It was dissolved in dimethylsulfoxide (DMSO) and diluted to achieve the desired concentrations before each experiment. The final concentration of DMSO in the culture medium was kept below 0.1%. Cell culture medium and fetal bovine serum were procured from Gibco (Grand Island, NY). Trypan blue, DMSO, propidium iodide (PI), Triton-X 100, RNase A and 1-(4,5-dimethylthiazol-2-yl)-2,5-diphenyl-tetrazolium bromide (MTT) were purchased from Sigma Chemical Co. (St. Louis, MO). Ethidium bromide (EtBr) and sodium

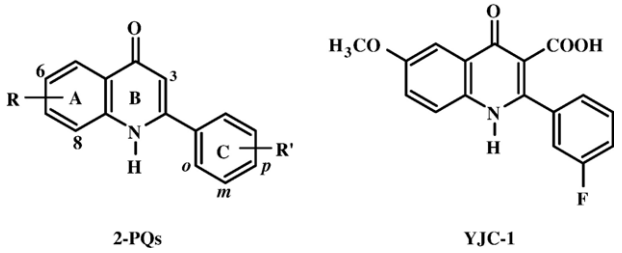

Fig. 1. Chemical structures of 2-PQs and YJC-1.

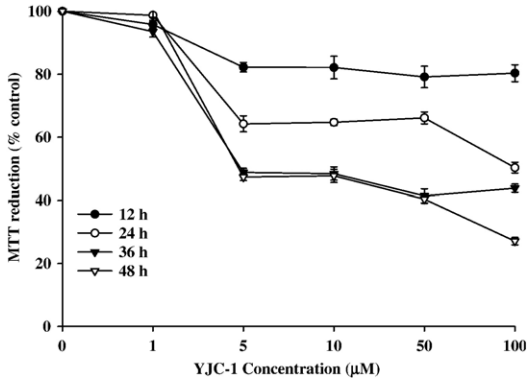

Fig. 2. Time and dose-dependent curves for YJC-1 in the MTT reduction assay. A549 cells were treated with YJC-1 at 1, 5, 10, 50 and 100 μM for 12, 24, 36 and 48 h. Data are expressed as means ± S.D. of three independent experiments.

dodecyl sulfate-polyacrylamide gel (SDS-PAGE) were from Bio-Rad Laboratories (Bio-Rad, CA). Nitrocellulose membranes were obtained from Amersham Pharmacia Biotech (Piscataway, NJ). Antibody against α-tubulin was from Santa Cruz Biotechnology (Santa Cruz, CA); antibody against phosphohistone H3 was from Cell Signaling Technology (Beverly, MA). The antibodies against CDK1, cyclin B1, $p21^{Cip1/Waf1}$, Cdc25C and p53 were from Upstate Biotechnology Inc. (Lake Placid, NY). Antibodies against β-actin and secondary antibodies were from Chemicon International, Inc. (Temecula, CA).

2.2. Cell culture

Human lung carcinoma A549 cells were obtained from the American Type Culture Collection (Manassas, VA) and grown in RPMI-1640 supplemented with 10% FBS, 1% dilution of penicillin-streptomycin and 1% L-glutamine and maintained at 37 °C in a humidified 95%–5% CO_2 atmosphere.

2.3. Cytotoxicity assay

Cytotoxicity was assessed using the MTT assay (Blagosklonny et al., 2002). A549 cells (5×10^3 cells/well in a 96-well plate) were treated without or with YJC-1 (1, 5, 10, 50 and 100 μM) for 12, 24, 36 and 48 h. After treatment, the relative cell proliferation was measured by scanning with an ELISA reader (Bio-Rad, CA) with a 570 nm filter.

2.4. Cell cycle distribution analysis

Cell cycle analysis by flow cytometry was performed as described in a previous paper (Hsu et al., 2005). A549 cells (1×10^5 cells/well) were treated with 5 μM YJC-1 for the indicated time periods. After treatment, cells were washed once with phosphate-buffered saline (PBS) and fixed with 70% ice-cold ethanol at −20 °C overnight. Then the cells were stained with a solution containing 1% Triton-X 100, 0.1 mg/ml RNase and 4 μg/mL PI in the dark for 30 min. Cell cycle distribution was measured using a FACScan flow cytometer (Becton Dickinson, San Jose, CA) and analyzed with Modfit software as described previously (Hsu et al., 2005).

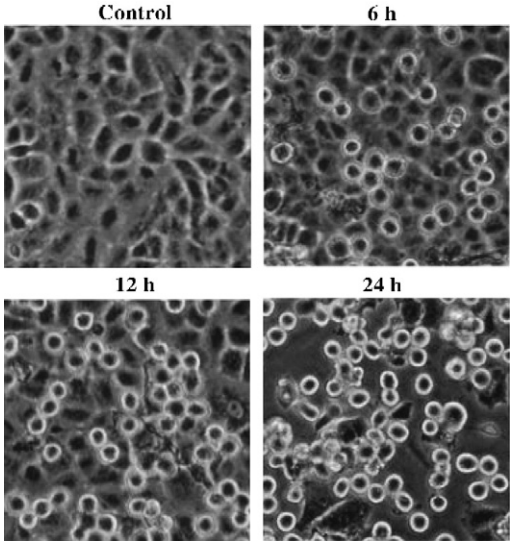

Fig. 3. YJC-1 induces mitotic morphological changes in A549 cells. After treatment with 5 μM YJC-1 for 6, 12 and 24 h, cells were observed under a phase-contrast microscope (magnification 200x).

2.5. Immunofluorescence microscopy

A549 cells (5×10^4 cells/well) plated on 4-well chamber slides were treated without or with 5 μM YJC-1 for 12 h. After treatment, cells were fixed in 4% formaldehyde in PBS for 15 min, permeabilized with 0.3% Triton-X 100 in PBS for 1 h with blocking of non-specific binding sites using 2% BSA. Fixed cells were then incubated with antihuman α-tubulin antibody (1:100 dilution) or phosphohistone H3 (1:100 dilution) overnight and then exposed to the secondary antibody (FITC-conjugated goat anti-mouse IgG at 1:100 dilution), followed by DNA staining with PI. Photomicrographs were obtained using a Leica TCS SP2 Confocal Spectral Microscope (Chen et al., 2002).

2.6. Western blot analysis

A549 cells (3×10^5 cells/well) were treated without or with 5 μM YJC-1 for the indicated time periods. After treatment, cells were washed once with PBS before M-PER® Mammalian Protein Extraction Reagent (PIERCE) was added to prepare a total cell lysate. Western blotting was conducted according to the procedures of Hodges and Chipman (2002). Approximately 20 μg of total cellular proteins were separated on 10 to 12% SDS-polyacrylamide gels which was then electrotransferred onto nitrocellulose membranes. The membrane was incubated with the desired primary antibody overnight at the following dilutions: CDK1 (1:1000), cyclin B1 (1:1000), Cdc25C (1:1000), $p21^{Cip1/Waf1}$ (1:1000), p53 (1:200), and β-actin (1:400). Subsequently, the membrane was incubated with appropriate secondary antibody, and the immunoreactive protein bands were visualized using enhanced chemiluminescence kit (Perkin-Elmer Life Sciences, Inc., Boston, MA) according to the manufacturer's instructions. Western blots are representative of at least two independent experiments.

2.7. Reverse transcription-polymerase chain reaction analysis (RT-PCR)

A549 cells (3×10^5 cells/well) were treated without or with 5 μM YJC-1 for the indicated time periods. Total RNA was isolated from cells using RNeasy® Mini Kit (Qiagen) as described in the previous paper (Hsu et al., 2005). RNA yields and purity were assessed by spectrophotometric analysis. Total RNA (5 μg) from each sample was subjected to reverse transcription with dNTPs in a total reaction volume of 12 μl. PCR was performed on cDNA, using *Taq* polymerase, dNTPs and the corresponding primers. Sequences for the $p21^{Cip1/Waf1}$ primers used in the PCR were forward 5′-TGCTGCCTGCT TCCCAGGAACA-3′ and reverse 5′-CCATCCCCTTCCTCACC TGAAA-3′. The resulting PCR products were analyzed on 1.5% agarose gels containing 0.5 μg/ml of EtBr as described previously (Hsu et al., 2005).

2.8. Tumor xenografts implantation

The protocol for measuring antitumor activity on tumor xenografts was performed as previously described (Wang et al., 2005). Male SCID mice (20 g, 4 weeks of age) were obtained from the Laboratory Animal Center of Medical College, National Taiwan University, and allowed to acclimate to laboratory conditions 1 week before tumor implantation. SCID mice were maintained in accordance with the Institutional Animal Care and Use Committee procedures and guidelines. A549 cells (1×10^7) were injected s.c. into the flank of each animal. When tumor reached an approximate volume of 60 mm^3, mice bearing tumors with acceptable morphology and of similar size range were selected and distributed for drug studies. A549 tumors were measured every 2–3 days using a caliper, and the body weight of the mice was monitored for toxicity. Tumor volumes were determined by measuring the length (l) and the width (w), and the volumes were calculated ($V=lw^2/2$) (Wang et al., 2005). The mice were killed when the tumor burden was over 1200 mg.

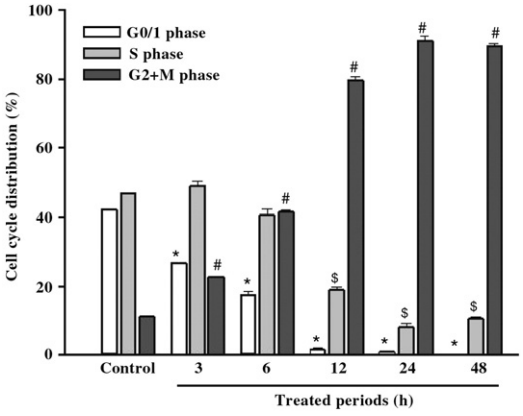

Fig. 4. YJC-1 induced G2+M phase arrest in A549 cells. After 5 μM YJC-1 treatment, the cells were harvested and fixed with cold 70% ethanol overnight then were stained with PI and the cell cycle distribution was measured by flow cytometry and analyzed by ModFit software. Data are expressed as means ± S.D. of three independent experiments. *, $P<0.001$; compared with the G0/1 phase of the control. $, $P<0.001$ compared with the S phase of the control; #, $P<0.001$; compared with the G2+M phase of the control.

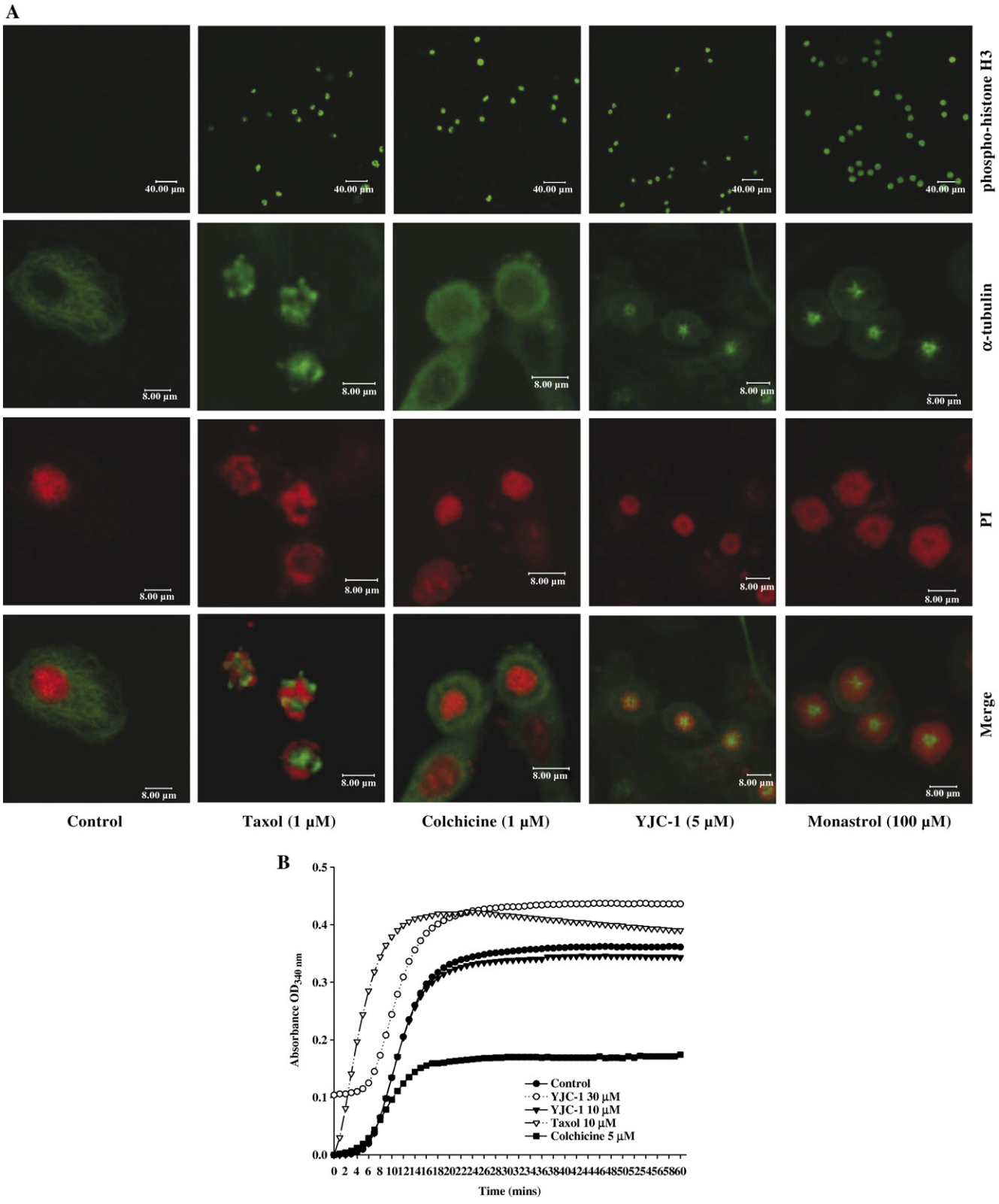

Fig. 5. YJC-1 induces microtubule stabilization in A549 cells. (A) Cells treated with paclitaxel, colchicine, YJC-1 or monastrol for 12 h were then fixed and stained with phosphohistone H3-FITC or double-stained with anti-α-tubulin-FITC and PI. They were examined under a Leica TCS SP2 Confocal Spectral Microscope. (B) Microtubule polymerization assay. Purified tubulins were used to assay microtubule formation *in vitro* in the presence of paclitaxel, colchicine or YJC-1. A shift of the curve upward to the up of the control represents an increase in polymerized microtubule. A shift to the downward represents a decrease in the rate of polymerization.

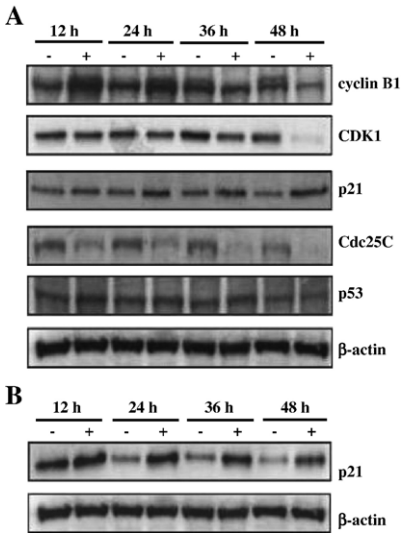

Fig. 6. Regulation of mitotic phase-associated proteins by YJC-1. (A) The expression of cyclin B1, CDK1, p21, Cdc25C and p53 after 5 μM YJC-1 treatment in A549 cells. (B) 2 μM YJC-1 induced the expression of $p21^{Cip1/Waf1}$ in p53-null cell line, HL-60 cells. β-actin antibody was used as an internal loading control.-/+: without/with YJC-1.

2.9. Statistic evaluation

Values are the means ± S.D. of three independent experiments. Student's *t* tests were used to assess the statistical significance of the differences, with "*P*" values of less than 0.05 being considered statistically significant.

3. Results

3.1. Inhibition of cell growth by YJC-1

The effect of YJC-1 on cell growth was examined at concentrations between 1 and 100 μM for 12, 24, 36 and 48 h. YJC-1 treatment exerted a concentration- and time-dependent inhibition of cell growth in A549 cells. The concentration required to inhibit cell growth by 50% (IC_{50}) was approximately 4.8 μM for the 48-h treatment (Fig. 2). Untreated cells grew in a monolayer, island-like manner that did not change even with a long incubation of 48 h. But cells exposed to YJC-1 exhibited a distinct rounded-up shape compared to the polygonal shape of controls and the changes were dependent on the length of the incubation (Fig. 3). When treatment was for 48 h, some apoptotic cells (cell shrinkage) were observed in YJC-1-treated cells (data not shown).

3.2. YJC-1 induces growth inhibition via arresting cell cycle at mitotic phase

The effect of cell cycle regulation was examined using flow cytometric analysis. YJC-1 exposure resulted in a significant increase in the number of cells in G2+M phase in a time-dependent manner. Exposure to 5 μM YJC-1 caused a blockade peaking at 24 h, with approximately 90% of cells in G2+M phase at that time compared to 10–13% in control cells. During prolonged treatment periods up to 48 h, most cells still remained in G2+M phase (Fig. 4). Because flow cytometric analysis cannot distinguish cells in G2 or M phase, we used phosphohistone H3 antibodies and PI staining to examine whether YJC-1 stopped the cell cycle in G2 or M phase. As illustrated in Fig. 5A, YJC-1-treated cells reacted with phosphohistone H3 antibodies and PI staining results showed that YJC-1 treatment significantly induced chromosomes condensation. We further investigated whether YJC-1 affected microtubule function. Spindle microtubules are shown by anti-α-tubulin immunofluorescence, and chromosomes are shown by PI staining. YJC-1-treated cells contained a ring of condensed chromosomes with a monopolar spindle pole in the center (ball-shaped spindle), similar to that seen with monastrol. Multipolar spindle poles have been detected in paclitaxel-treated cells. In contrast, exposure to colchicine resulted in distinct microtubule depolymerization. According to the results of microtubule stabilization experiments, taxol caused significant microtubule stabilization and colchicine caused significant microtubule destabilization, compared with control. However, YJC-1 did not significantly affect microtubule stabilization (Fig. 5B). Exposure to either a low (10 μM) or a high (30 μM) concentration of YJC-1 resulted in curves for YJC-1 similar to that of control. Although the curve for 30 μM YJC-1 ended and started higher than that of control.

3.3. Expression of cell cycle regulatory proteins

The effect of YJC-1 on the expression of cell cycle regulator proteins was determined by immunoblot. YJC-1 treatment induced an early increase in cyclin B1 within 12–24 h, but a detectable reduction was observed at 36–48 h. The expression of CDK1 underwent no detectable change within 12–24 h, but decreased at 36–48 h (Fig. 6A). To further determine the mechanism by which CDK1 is regulated by YJC-1, we examined the upstream regulators of CDK1. YJC-1 induced a time-dependent increase in $p21^{Cip1/Waf1}$, whereas a decrease in Cdc25C was observed. However, treatment with YJC-1 did not affect the expression of p53 (Fig. 6A). In addition, YJC-1 also

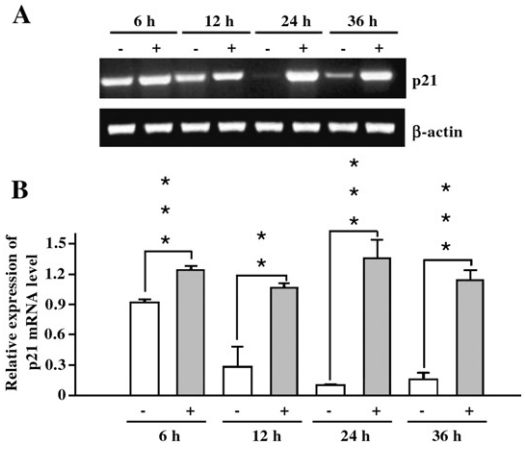

Fig. 7. Effect of YJC-1 on the transcription of $p21^{Cip1/Waf1}$ in A549 cells. (A) The expression of p21 after 5 μM YJC-1 treatment for the indicated time periods. (B) Quantitative $p21^{Cip1/Waf1}$ expression after normalization to β-actin. **, $P<0.01$; ***, $P<0.001$; compared with the negative control.-/+: without/with YJC-1.

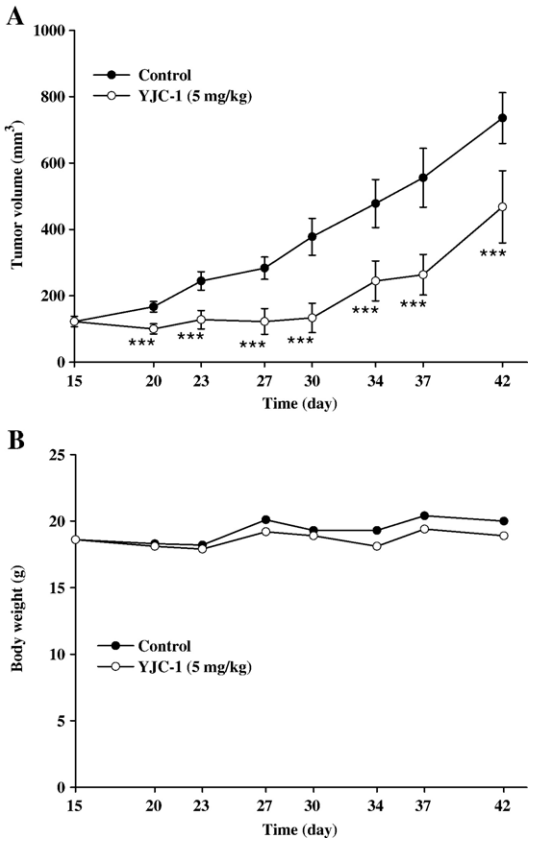

Fig. 8. Effect of YJC-1 on tumor cell growth in an *in vivo* model. (A) The tumor volume effect. (B) The body weight effect. Data are expressed as means ± S.D. of three independent experiments. ***, $P<0.001$; compared with the control.

induced the expression of $p21^{Cip1/Waf1}$ in HL-60 cells (p53-null) and the effect was time dependent (Fig. 6B).

3.4. Reverse transcription-polymerase chain reaction analysis

We also analyzed the transcriptional expression of related cell cycle regulatory genes. YJC-1 induced a profound elevation in $p21^{Cip1/Waf1}$ gene expression (Fig. 7), but did not affect the expression of other genes (data not shown).

3.5. Antitumor cell growth activity of YJC-1 on A549 tumor xenografts

On the basis of the significant growth-inhibitory effect of YJC-1 *in vitro*, we investigated whether YJC-1 possessed antitumor cell growth activity *in vivo*. YJC-1 (5 mg/kg) inhibited tumor growth in the period from 20 to 42 days (Fig. 8A), indicating the *in vivo* efficacy of orally administered YJC-1. In addition, we observed little difference in body weight between control and YJC-1-treated animals (Fig. 8B), indicating that YJC-1 had minimal toxicity *in vivo*.

4. Discussion

2-PQ derivatives have been identified as antimitotic agents, and their structure-activity relationships have been discussed. However, all of these effective compounds are too lipophilic to be optimal for *in vivo* and clinical studies. Thus, we tried to introduce a carboxylic acid group into the 2-PQ skeleton to improve the pharmacokinetic properties of these cytotoxic compounds. Among these 3-carboxylic acid derivatives, only compounds that contain a fluorine atom at the *m*-position of the 2-phenyl group showed significant activity. YJC-1 was the most potent compound. However, cytotoxicity decreased when the *m*-position of the 2-phenyl group was substituted with OCH_3, Cl or H rather than F (Lai et al., 2005). In this study, we determined that YJC-1 had an antitumor effect via mitotic phase arrest in A549 cells. This finding confirms previously reported studies indicating that 2-PQ derivatives arrest cell growth in the mitotic phase (Kuo et al., 1993; Li et al., 1994a,b; Chen et al., 1997; Xia et al., 1998, 2003; Hadjeri et al., 2004; Lai et al., 2005).

Because site-specific phosphorylation of histone H3 is a marker for mitotic progression in mammalian cells (Prigent and Dimitrov, 2003), we used phosphohistone H3 antibodies and PI staining to examine whether YJC-1 arrests the cell cycle in M phase. YJC-1 treatment caused cells to round-up, and chromosomes to condense and become responsive to phosphohistone H3 antibodies, findings which show that YJC-1 induces mitotic phase arrest. Spindle microtubules and chromosome staining revealed that YJC-1 treatment caused a ball-shaped spindle which presumably failed in centrosomal duplication or separation. Such ball-shaped spindles have been observed in cells treated with monastrol, which induces microtubule polymerization (Marcus et al., 2005). Multipolar spindles occurred after treatment with the stabilizing drug, taxol; however, exposure to the destabilizing drug, colchicines, resulted in microtubule deploymerization. In addition, microtubule stabilization experiments also verified the above observations. Taxol caused significant microtubule stabilization and colchicine caused significant microtubule destabilization, compared with control. However, YJC-1 did not affect microtubule stabilization. Thus, we suggest that YJC-1 perturbed the mitotic spindle, leading to a ball-shaped spindle (similar to that seen with the stabilizing agent monastrol), but it does not affect microtubule stability.

Cyclin B and CDK1 are intricately involved in cell-cycle progression through the G2+M phase transition (Stewart et al., 2003). YJC-1 treatment induced an earlier increase in cyclin B1 within 12–24 h, but a detectable reduction was observed at 36–48 h. In addition, YJC-1-treatment decreased the expression of CDK1 and Cdc25C. These finding suggest that Cdc25C is involved in the regulation of CDK1/cyclin B1 activity in YJC-1 treated A549 cells. P21 is known to be up-regulated by p53, both of which are integrated in G1 and G2 arrest machinery in response to DNA damage (el-Deiry et al., 1993; Arima et al., 2004). Exposure to YJC-1 induced a remarkable increase in the protein and mRNA levels of $p21^{Cip1/Waf1}$ at all times investigated but did not induce a significant change in the expression of p53. In addition, YJC-1 also caused a significant elevation in $p21^{Cip1/Waf1}$ expression in p53-null cell line, HL-60 cells (Fig. 6B). These findings demonstrated that YJC-1-induced $p21^{Cip1/Waf1}$ expression could occur via a p53-

independent pathway. Indeed, Choi et al. (2000) have demonstrated that p53-independent induction of p21 by the isoflavone genistein leads to cell cycle arrest in the G2+M phase. In an *in vivo* study, YJC-1 inhibited tumor growth with minimal toxicity.

In summary, we have demonstrated that exposure of A549 cells to YJC-1 results in cell cycle arrest. YJC-1 treatment induced mitotic phase arrest via chromosome condensation with a monopolar spindle pole array formation. This affects the cell cycle regulation process by inducing elevated or suppressed expression of many proteins via a p53-independent pathway.

Acknowledgement

The investigation was supported by research grants from the National Science Council of the Republic of China (NSC92-2323-B-039-001 and NSC95-2320-B-039-011-MY3) awarded to S.C. Kuo and L.J. Huang.

References

Arima, Y., Hirota, T., Bronner, C., Mousli, M., Fujiwara, T., Niwa, S., Ishikawa, H., Saya, H., 2004. Down-regulation of nuclear protein ICBP90 by p53/p21$^{Cip1/Waf1}$-dependent DNA-damage checkpoint signals contributes to cell cycle arrest at G1/S transition. Genes Cells 9, 131–142.

Bacher, G., Beckers, T., Emig, P., Klenner, T., Kutscher, B., Nickel, B., 2001. New small-molecule tubulin inhibitors. Pure Appl. Chem. 73, 1459–1464.

Blagosklonny, M.V., Robey, R., Sackett, D.L., Traganos, F., Darzykiewicz, Z., Fojo, T., Bates, S.E., 2002. Histone deacetylase inhibitors all induce p21 but differentially cause tubulin acetylation, mitotic arrest, and cytotoxicity. Mol. Cancer Ther. 1, 937–941.

Chen, K., Kuo, S.C., Hsieh, M.C., Mauger, A., Lin, C.M., Hamel, E., Lee, K.H., 1997. Antitumor agents. 174. 2′,3′,4′,5,6,7-Substituted 2-phenyl-1,8-naphthyridin-4-ones: their synthesis, cytotoxicity, and inhibition of tubulin polymerization. J. Med. Chem. 40, 2266–2275.

Chen, Y.N., Chen, J.C., Yin, S.C., Wang, G.S., Tsauer, W., Hsu, S.F., Hsu, S.L., 2002. Effector mechanisms of norcantharidin-induced mitotic arrest and apoptosis in human hepatoma cells. Int. J. Cancer. 100, 158–165.

Choi, Y.H., Lee, W.H., Park, K.Y., Zhang, L., 2000. p53-independent induction of p21 (WAF1/ CIP1), reduction of cyclin B1 and G2/M arrest by the isoflavone genistein in human prostate carcinoma cells. Jpn. J. Cancer Res. 91, 164–173.

Department of Health, 2005. Vital Statistics, 2004. Department of Health, Taipei.

el-Deiry, W.S., Tokino, T., Velculescu, V.E., Levy, D.B., Parsons, R., Trent, J.M., Lin, D., Mercer, W.E., Kinzler, K.W., Vogelstein, B., 1993. WAF1, a potential mediator of p53 tumor suppression. Cell 75, 817–825.

Hadjeri, M., Peiller, E.L., Beney, C., Deka, N., Lawson, M.A., Dumontet, C., Boumendjel, A., 2004. Antimitotic activity of 5-hydroxy-7-methoxy-2-phenyl-4-quinolones. J. Med. Chem. 47, 4964–4970.

Hodges, N.J., Chipman, J.K., 2002. Down-regulation of the DNA-repair endonuclease 8-oxo-guanine DNA glycosylase 1 (hOGG1) by sodium dichromate in cultured human A549 lung carcinoma cells. Carcinogenesis 23, 55–60.

Hsu, M.H., Kuo, S.C., Chen, C.J., Chung, J.G., Lai, Y.Y., Huang, L.J., 2005. 1-(3,4-Dimethoxy-phenyl)-3,5-dodecenedione (I6) induces G1 arrest and apoptosis in human promyelocytic leukemia HL-60 cells. Leuk. Res. 29, 1399–1406.

Igor, B.R., 2003. Tumor cell senescence in cancer treatment. Cancer Res. 63, 2705–2715.

Jemal, A., Murry, T., Ward, E., Samuels, A., Tiwari, R.C., Ghafoor, A., Feuer, E.J., Thun, M.J., 2005. Cancer statistics, 2005. CA Cancer J. Clin. 55, 10–30.

Kuo, S.C., Lee, H.Z., Juang, J.P., Lin, Y.T., Wu, T.S., Chang, J.J., Lednicer, D., Paull, K.D., Lin, C.M., Hamel, E., 1993. Synthesis and cytotoxicity of 1,6,7,8-substituted 2-(4′-substituted phenyl)-4-quinolones and related compounds: identification as anti-mitotic agents interacting with tubulin. J. Med. Chem. 36, 1146–1156.

Lai, Y.Y., Huang, L.J., Lee, K.H., Xiao, Z., Bastow, K.F., Yamori, T., Kuo, S.C., 2005. Synthesis and biological relationships of 3′,6-substituted 2-phenyl-4-quinolone-3-carboxylic acid derivatives as antimitotic agents. Bioorg. Med. Chem. 13, 265–275.

Larsen, A.K., Escargueil, A.E., Skladanowski, A., 2003. Catalytic topoisomerase II inhibitors in cancer therapy. Pharmacol. Ther. 99, 167–181.

Li, L., Wang, H.K., Kuo, S.C., Wu, T.S., Lednicer, D., Lin, C.M., Hamel, E., Lee, K.H., 1994a. Antitumor agents. 150. 2′,3′,4′,5′,5,6,7-substituted 2-phenyl-4-quinolones and related compounds: their synthesis, cytotoxicity, and inhibition of tubulin polymerization. J. Med. Chem. 37, 1126–1135.

Li, L., Wang, H.K., Kuo, S.C., Wu, T.S., Mauger, A., Lin, C.M., Hamel, E., Lee, K.H., 1994b. Antitumor agents. 155. Synthesis and biological evaluation of 3′,6,7-substituted 2-phenyl-4-quinolones as antimicrotubule agents. J. Med. Chem. 37, 3400–3407.

Marcos, M., Mariano, B., 2001. To cycle or not to cycle: a critical decision in cancer. Nat. Rev. 1, 222–231.

Marcus, A.I., Peters, U., Thomas, S.L., Garrett, S., Zelnak, A., Kapoor, T.M., Giannakakou, P., 2005. Mitotic kinesin inhibitors induce mitotic arrest and cell death in Taxol-resistant and-sensitive cancer cells. J. Biol. Chem. 280, 11569–11577.

Osterlind, K., 2001. Chemotherapy in small cell lung cancer. Eur. Respir. J. 18, 1026–1043.

Owa, T., Yoshino, H., Yoshimatsu, K., Nagasu, T., 2001. Cell cycle regulation in the G1 phase: a promising target for the development of new chemotherapeutic anticancer agents. Curr. Med. Chem. 8, 1487–1503.

Pizzolato, J.F., Saltz, L.B., 2003. The camptothecins. Lancet 28, 2235–2242.

Prigent, C., Dimitrov, S., 2003. Phosphorylation of serine 10 in histone H3, what for? J. Cell Sci. 116, 3677–3685.

Sandal, T., 2004. Molecular aspects of the mammalian cell cycle and cancer. Oncologist 7, 73–81.

Shapiro, G.I., Harper, J.W., 1999. Anticancer drug targets: cell cycle and checkpoint control. J. Clin. Invest. 104, 1645–1653.

Stewart, Z.A., Westfall, M.D., Pietenpol, J.A., 2003. Cell-cycle dysregulation and anticancer therapy. Trends Pharmacol. Sci. 24, 139–145.

Wang, S.W., Pan, S.L., Guh, J.H., Chen, H.L., Huang, D.M., Chang, Y.L., Kuo, S.C., Lee, F.Y., Teng, C.M., 2005. YC-1 [3-(5′-hydroxymethyl-2′-furyl)-1-benzyl-indazole] exhibits a novel antiproliferative effect and arrests the cell cycle in G_0-G_1 in human hepatocellular carcinoma cells. J. Pharmacol. Exp. Ther. 312, 917–925.

Xia, Y., Yang, Z.Y., Xia, P., Bastow, K.F., Tachibana, Y., Kuo, S.C., Hamel, E., Hackl, T., Lee, K.H., 1998. Antitumor agents. 181. Synthesis and biological evaluation of 6,7,2′,3′,4′-substituted-1,2,3,4-tetrahydro-2-phenyl-4-quinolones as a new class of antimitotic antitumor agents. J. Med. Chem. 41, 1155–1162.

Xia, Y., Yang, Z.Y., Xia, P., Bastow, K.F., Nakanishi, Y., Nampoothiri, P., Hamel, E., Brossi, A., Lee, K.H., 2003. Antitumor agents. Part 226: synthesis and cytotoxicity of 2-phenyl-4-quinolone acetic acids and their esters. Bioorg. Med. Chem. Lett. 13, 2891–2893.